國立清華大學生命科學系

碩士論文

矽藻(*Skeletonema costatum*)中矽沈積相關蛋白

Silica Deposition Associated Proteins in Diatoms

(*Skeletonema costatum*)

學生：石清華

指導教授：李家維 教授

民國九十二年 六月 二十一日

摘要

由生物合成的無機構造，稱之為生物礦物，在自然界中是一個廣為分佈的現象。能夠產生生物礦化的有機體利用著有機分子來產生各式各樣的構型。而矽藻的生物矽展現了令人讚嘆的多樣化構型：由奈米至微米大小所架構出的種專一性的構型。在矽藻細胞壁的形成過程中，沈積的矽產生三種的型態：作為球顆粒、作為六角柱、以及作為細絲狀。在先前的研究中，證實由在許多的矽藻細胞壁的氟化氫萃取物能夠在無機的環境下促使矽沈積的構型成為球顆粒。在此，我們的工作展示了在另一矽藻種 *Skeletonema costatum* 的細胞壁氟化氫萃取物可以促使矽沈積在無機的環境下成為另一種構型，細絲狀。

Abstract

The biological formation of inorganic structures, termed biominerals, is a widespread phenomenon in nature. Biomineraling organisms use organic molecules to generate species-specific patterns. Diatom biosilica displays a dazzling variety of species-specific silica patterns that are structured on a nanometer-to-micrometer scale. Deposited silica occurs in three morphological forms in the wall formation: as spherical particles, as hexagonal columns, and as microfibrils. Previous studies demonstrated that HF-extract of cell wall of numerous diatom species can direct the silica deposition as spherical particles *in vitro*. Here, we demonstrate HF-extract of cell wall of *Skeletonema costatum* can direct silica deposition as another form, microfibrils.

誌 謝

時序芒苒，又一次走到了夏天。

算算日子，待在清華，這個與我同名的地方，也有六年。進李家維老師的實驗室，是在大學二年級的時候，而今已經是碩士畢業。時間總是走得太匆匆，許多高聲歡笑、許多深沈難過根本來不及察覺就已經消逝，所留下的只有偶然與其他人命運交錯下所產生的回憶。

很想套用陳之藩的一句話：要謝的人太多，要謝就謝天吧。然而，我還是很想逐一表示謝意。很感激李家維老師能夠接納大二對於實驗室一無所知的我進入實驗室來學習，直至現在，五年歲月，長年的指導是無可言喻的。汶吉、和昇、寧寧，大學時共同合作的學長姐，由於你們的照顧與指導，讓我學了不少。華子，相當感謝妳在實驗上的一些意見建議，以及在實驗之外對大家的照顧。鈺婷，聰明但是常常思路搭錯線的同學，總是能夠創造出笑話，為實驗室的生活添加許多色彩。貞祥，總是辛苦地幫大家買便當。此外，慧毅、介輔、馥菱、怡靜、靜怡、懿慧，許許多多的實驗室成員，來來去去之間共同增添了回憶。圍繞在我身邊的朋友們、一同學習的同學、偶爾一起聊天想著奇怪的事情的朋友、教我油畫的老師，能夠與你們時光共同交錯，實在是一件喜悅的事情。

在清華的日子，一段不算短的日子，校園還是美麗，人來人往依舊。對我而言，清華其實是沒什麼改變的，只是走慣的夜間的校園變得明亮，平常仰望的星空因此變得黯淡許多。到了別離的時候，將承襲著大家對我的改變，離去。

Content

I. Introduction

The living world is full of specialized inorganic materials, including shells and coral made from calcium carbonate, ivory, enamel and bone made from calcium phosphates, and magnetic sensing devices and radular teeth made from iron oxides [1]. Diatoms, sponges and some plant parts are made from silica. Exquisite structures such as shells, spines, fibers and granules in many protests, diatoms, sponges, mollusks and higher plants composed by amorphous silica, the simplest siloxane $[(SiO_2)_n]$ are constructed under mild physiological conditions [2].

Diatom protoplast is enveloped by a cell wall comprising organic components and a large amount of silica. The siliceous component is known as "the frustule." While cell are not dividing, the frustule consists of two hemicylindrical halves denoted as "valves" and a number of incomplete siliceous rings termed girdle bands. The valves differ in size, the larger one is termed as "epitheca", and the smaller one is termed as "hypotheca". The asexual reproduction divides one cell into two, with each valve of the parent cell becoming an epitheca of the daughter cell [7]. New valve formation has been studied in detail by a number of researchers utilizing thin sections and transmission electron microscopy [3, 4, 5, 6, 7, 8], and observed extensively in numerous diatom species at the ultrastructural level. A rather complete description is summarized by Zurzolo and Bowler [9].

Drum and Pankratz [10, 11], Stoermer et al [12], Dawson [13], and Pickett-Heaps and Kowalski [14] described the early stage of silica deposition as consisting of a feathery structure or of gradually thickening microfibrils. Borowitzka and Volcani [15], and

Schmid and Schulz [16] reported the presence an assemblage of silica spheres during wall formation. Deposited silica occurs in three morphological forms in the wall formation of *Ditylum brightwell*: as homogeneous base layer, as hexagonal columns, and as microfibrils [17]. The base layer is continuous thin structure and is the form in which silica is first deposited in every part of the siliceous wall. The initial thickness of the thin layer is about 14 nm on the outer tube of the labiate process and about 7 nm on the valve face, the marginal ridge, the valve mantle, and the girdle bands. The thin layers can increase its thickness by deposition of amorphous silica reaching about 90 nm on the valve face. Hexagonal columns occur on the outside of the outer tube of the labiate process. Deposition of amorphous silica increases the height of the columns and gradually fills the spaces between the columns. Siliceous microfibrils occur on the outside of the outer tube of the labiate process, on the inside of the valve face and valve mantle, and on the whole surface of the marginal ridge. Deposition of amorphous silica gradually solidifies the microfibrils. No siliceous silica spherical structure was found in wall formation of *D. brightwellii*, but the possibility that siliceous spheres exist in this diatom is not excluded, since the smallest unit of silica particles can aggregate to form larger particles, *e. g.*, 1.5 nm and 10 nm [18].

Cell wall formation in diatoms involves two different major processes: (1) the synthesis of the organic components of the frustule, and (2) the transport and polymerization of silicic acid [$Si(OH)_4^{2-}$] and deposit as silica $(SiO_2)_n \bullet nH_2O$. The stages of wall formation include DNA replication, mitosis, and cytokensis; the appearance of microtubules and the migration of the nucleus; the appearance of silica deposition vesicles (SDV), the initiation of silica deposition, and formation of the new valves; the formation of girdle bands; the appearance of organic casing and some addition of secondary organic material; and finally, cell separation [19, 20].

The deposition of new siliceous valves between mitosis and daughter cell separation requires precise coupling between silicon metabolism and the cell cycle [21]. It has been observed in several species that silica uptake precedes cell division [22]. The strict requirement for silica in frustule formation has led to the evolution of silica-dependent checkpoints in diatom mitosis. Two arrest points appear universal in different diatom species, one at the G1/S boundary and another during G2/M associated with the construction of new valve [23, 24]. The arrest point at G1/S has been proposed to be the indicative of a silica dependency for DNA synthesis, and this block serves to determine whether sufficient silica is available to complete frustule biogenesis [25, 26].

A common feature of biominerals is their associated macromolecules. Silaffins together with polyamines bind the silica scaffold extremely tightly and can only be removed following solubilization of silica with anhydrous hydrogen fluoride (HF). Siliaffins, which are cationic peptides, isolated from purified cell walls of the diatom *Cylindrotheca fusiformis* were shown to generate networks of silica nanospheres within seconds when added to a solution of silicic acid [27]. Silafin-1 contains a previously undescribed type of protein modification, polyamine. A polyamine consisting of 6-11 repeats of the *N*-methyl-propylamine unit covalently attached to specific lysine residues [27]. *Cylindrotheca fusiformis* contains two major types of silaffins, denoted silaffin-1A (4kDa) and silaffin-1B (8kDa). Both are proteolytically derived from the product of a single gene, *Sil1*.

Kröger et al [28] analyzed the HF-extractable organic cell wall components from a wide range of diatom species and found that the cell wall of each diatom contains not

only a species-specific set of silica-precipitating proteins (silaffins) but also high amounts of long-chain polyamines. These polyamines occur in species-specific variations [28]. When these polyamines are added to a silicic acid solution in vitro, a precipitate forms after a few minutes that is composed of both silica and polyamines. The precipitate contains 1.25 µg SiO_2 per 1 µg of polyamine. The stoichiometry suggests a tight interaction between the amino groups and the silanol groups of silica. Hydrogen bonding interaction has been demonstrated for silica gel/amine hybrids that are composed of silica and synthetic polyallylamine [29]. Polyamines are known to accelerate silicic acid polymerization [30]. The positively charged polyamines interconnect negatively charged polysilicic acid particles by simultaneous electrostatic interactions on adjacent particles [31].

Silica appears to be deposited in different forms during valve morphogenesis. Especially evident was the precipitation of silica spheres ranging up to 100 nm in diameter [32,33]. Both the silaffins and polyamines can promote silica precipitation *in vitro*, generating a network of nanospheres with diameters between 100nm and 1µm, depending on the molecules used and the pH environment of the solution [27, 28]. When polyamines in the mass range of 1000 to 1250 Da are added to silicic acid solution at pH 5.0, the precipitate forms silica spherical particles. These aggregates are dominated by spheres of 800 nm – 1 µm in diameter. At the surfaces of the large spheres, smaller spheres are attached with diameters of only 100 – 200 nm. If polyamine mass ranges between 600 to 700 Da, the 100 – 200 nm spheres dominate.

HF-extractable material also contains fractions of high molecular mass, denoted as pleuralins [34,35]. Pleuralin-1 is specifically localized to the terminal girdle band of the epitheca. It is also targeted to the girdle band of the hypotheca of a cell

undergoing mitotic division process [36]. Pleuralin-1 is not targeted to the SDV but is directly secreted into the cleavage furrow [36]. Exocytosis is thought to involve in the transport of pleualin-1.

Calcium-binding glycoproteins known as frustulins [37] have been localized to the outer coating of diatom cell walls. The frustulins are localized ubiquitously over the external surface of the cell wall [34, 37]. Because they are not an integral component of the siliceous cell wall, they are not thought to participate in the silica biomineralization process. Five different types of frustulins have been described: α-frustulin (75-kDa), β-frustulin (105-kDa), γ-frustulin (140-kDa), δ-frustulin (200-kDa), and ε-frustulin (35-kDa).

Silaffins, frustulins, and pleuralins are all synthesized as precursor proteins containing *N*-terminal signal sequences for co-transcriptional import of proteins into the endoplasmatic reticulum. Other unidentified sequences are likely to be present within the silaffin and frustulin precursors that target them from the Golgi apparatus to the SDV [19].

As a result of extensive studies, it is now known that biological systems use (glycol)proteins to establish control over mineral nucleation and growth to synthesize materials of specific size, structure, shape, and orientation. The proposed mechanisms of control have been extensively reviewed [39, 40].

Diatom biosilica displays a dazzling variety of species-specific silica structures in nanometer scale [41, 42]. Previous studies focused on cell wall biogenesis in a number of diatoms species led to the conclusion that silica appears to deposit in

different forms during valve morphogenesis. Especially evident was the participation of silica spheres ranging up to 100 nm in diameter during production of cell wall [32, 42]. Elucidating mechanisms controlling production of nanostructured biosilica is a fascinating biochemical issue, and also is of great interest in material chemistry. So far, the industrial synthesis of silica sphere requires either strongly alkaline conditions [30] or high temperatures and long incubation times [43 44]. Biomimetic approaches are believed to allow the production of advanced materials at ambient temperature and with high precision, which are expected to exhibit superior properties in a wide range of application [45]. These biologically produced silica exhibit a genetically controlled precision of nanoscale architecture that exceeds the capacities of current-day human engineering. Biotechnological approaches are now starting to unlock the molecular mechanisms of polysiloxane synthesis under physiological conditions, offering the prospect of new, environmentally benign routes to the synthesis and structural control of these important materials [46, 47].

Here, we demonstrate that the biosilica extracts of diatom, *Skeletonema costatum*, can accelerate and control the process of silica formation in an *in vitro* condition. However, in biological organisms, additional controls must be exerted during the formation of silica precipitation. Much remains to be investigated in further research to understand the mechanisms how biological organisms regulate mineral formation. The information obtained will not only reveal the secrets of silicon deposition in organisms, but also assist us in our understanding in the generation of new materials with specific form and function for industrial application.

II. Materials and Methods

(A) Materials

The diatom, *Skeletonema costarum*, is kindly provided by Taiwan Fishery Research Institute.

(B) Methods

(1) Preparation of Silica Shells

When *Skeletonema costarum* reaches the maximum amount of the growth curve, each batch is concentrated from 3000L into 5L. Homogenize the diatom on ice and recover the frustules by centrifugation with 2800 g for 30 min at 4℃. A batch of frustules is boiled with 1L 2% SDS/100mM EDTA solution for 10 min twice to remove the intracellular components which may be attached on the frustule surface. Wash with acetone to remove the surfactant and any possible remaining intracellular component, and then wash with H_2O extensively. Frustules are lyophilized, and stored at -20℃.

(2) Extraction of Silica Deposition Associated Components

Weight 10 mg silica shell, and treat silica shell with 10 mL 2M HF/ 4M NH_4F on ice for 4 hours and shake them gently. Certifugate the mixture with 10k r.p.m. for 10 min. Collect the supernatant and use it to the following experiments immediately.

(3) SDS-Polyacrylaminde Gel Electrophroesis

The electrophoresis is carried out with 12% separating gel and 4% stacking

gel. The procedure of the electrophroesis is referred to the discontinuous buffer system perposed by Laemmli [48]. Silver staining is utilized to detect the existence of the protein.

(4) Chromatography

The column is packed with Sephacryl S-200 (Pharmacia Biotech). The column is eluted with 10 mM sodium acetate. Collect each fraction every 10 mL.

(5) Dialysis

The dialysis membrane (Spectra/Por) has the molecular weight cut off (MWCO) 1000 Da. Dialysis is against 10 mM sodium acetate for 24 hours with two exchanges. The procedures are carried out at 4℃.

(6) Scanning Electron Microscopy and Sample Preparation

Mix the biosilica extract with 0.01M and 0.01mM Na_2SiO_3, pH 3. Keep the mixture on ice, and vortex it gently. Spin down the mixture and remove the supernatant.

Alcohol series 20%, 30%, 50%, 75%, 90%, 100%, and 100% are utilized to remove H_2O. Following alcohol series, critical point dehydration (CPD, Hitachi HCP-2) is carried out. Coat the sample with Au or Pt. Samples are observed within SEM (Hitachi S-470). Moreover, EDX (Horiba EX-300) is carried out for element analysis.

III. Results

(A) Extraction of the silica associated components.

Treatment with 2M HF/ 4M NH_4F on ice will dissolute silica and release the associated organic components. These components contain proteins, with the molecular weights 70.4, 59.4, 56.8, 46.8, 39.3, 31.2, 27.5, 26.0, 25.0, 22.7, 19.1, 18.0, and 16.1 kDa. The SDS-PAGE is shown in Figure 1. Four proteins with dominant quantity are 56.8, 46.8, 39.3, and 31.2 kDa. Small proteins with the molecular weights less than 30 kDa show less quantity. Although 4M HF treatment can dissolute the biosilica, this method will destroy parts of the proteins. Moreover, these organic components are lost after dialysis (Figure 1).

(B) Purification by Chromatography

All fractions of gel filtration do not give any band in SDS-PAGE. The concentrated fractions still show no result in SDS-PAGE.

(C) Silica Deposition

The dry weight of silica deposition with time sequences 10 min, 30 min, 60 min, 90 min, 120 min, 3 hr, 6 hr is shown in Table 1. The dry weight of silica deposition increases from 0.08323 g (10 min) to 0.10023 g (6 hr), however, the system error is 0.011331 g.

(D) Scanning Electron Microscopy

Mostly, the silica deposition patterns are fibrils and plates. At acidic condition, pH 3, the fibrils have similar size in diameter with the time sequences 10 min, 20 min, 30 min, 60 min, 90 min, 120 min, 3 hr, 6 hr, 9 hr, 12 hr, and 24 hr (Figure 2-6). The diameters are summarized in Table 2. Not all fibrils are formed in random directions. A bundle of fibrils, arrays of fibrils, and stacks of these arrays exist. Silica deposition has the same pattern when the deposition time is 48 hr and 72 hr (data of 20 min, 90 min, 120 min, 3 hr, 9 hr, 12 hr, 48 hr, and 72 hr are not shown).

Besides fibril, plates are also observed. Most of the plates show a smooth surface. However, some show a discontinuous surface. The detail structures show stacks of thin layers, which have the thickness 47.49 nm (std. 3.07 nm). Each layer is composed with arrays of fibrils and can be observed clearly (Figure 6). When the pH environment changes from pH 3 to pH 7, the same fibril pattern is also observed under SEM.

Amazing patterns are also observed. While treating silica shell with 1M HF/ 2M NH_4F for 4 hours, and then dialyzed against ddH_2O, bilateral symmetrical, leaf-shape small plates can be formed. They are 2.5 μm in length and 0.75 μm in width. There are fine structures on these plates surface (Figure 7).

(E) EDX

The signals of Si and Au are overlapping in EDX analysis. Thus, little of none Si signal can be detected if the samples are coated with Au. Pt and Si have distinct signal spectra and therefore, strong Si signal can be detected. Besides Pt, Si, O, and C, EDX shows no other signal existing (Figure 8).

IV. Discussion

The SDS-PAGE shows that there are lots of proteins within the extract of the biosilica. These components contain proteins, with the molecular weights 70.4, 59.4, 56.8, 46.8, 39.3, 31.2, 27.5, 26.0, 25.0, 22.7, 19.1, 18.0, and 16.1 kDa. Four proteins with dominant quantity are 56.8, 46.8, 39.3, and 31.2 kDa. Small proteins with the molecular weights less than 30 kDa show less quantity. The silaffins in *C. fusiformis* have the molecular weight less than 10 kDa, and have long chain polyamine modification. Each polyamine modification will increases molecular weight of silaffins by about 1 kDa depending upon the chain length. The differences of molecular weight spectrum of the associated organic components between two diatom species, *S. costatum* and *C. fusiformis*, may be due to differential polyamine modification and species differences. However, these proteins in *S. costatum* seem to be less stable. No protein signal can be detected in gel filtration. All fractions concentrated by lyophilization do not have any band in SDS-PAGE. These components will disappear even under -20℃ storage. Avoiding loss of proteins, we carried out the following experiments by utilizing the crude extract.

Dissolution of silica with HF has been used for years. However, HF treatment is known to cleave *O*-glycosidic and phosphate ester bonds. And so, *O*-glycosidic modifications will be destroyed under this treatment. A mild extracting condition with HF and NH_4F, which NH_4F acts as a buffer, will slow down the reactions and prevent to destroy the modifications of proteins.

In *C. fusiformis*, silaffin-1A has both long chain polyamines and highly

phosphorylation modification. The zwitterionic structure of native silaffins enables the formation of supremalocular assemblies. Time-resolved analysis of morphogenesis of silica deposition *in vitro* detected a plastic silaffin-silica phase, which may represent a building material of diatom biosilica. It also shows that the morphogenesis of silica deposition may complete fast, in this case, less than 10 min.

The dry weight of silica deposition increases from 0.08323 g (10 min) to 0.10023 g (6 hr), however, the system error is 0.011331 g. Since the system error is 0.011331 g, we conclude that the total amount of silica deposition may be completed within 10 min, and little silica deposition process occurs while deposition time is longer than 10 min. This observation is just consistent with the previous studies.

At pH 3, silica deposition generates fibril patterns. With different deposition time, these fibrils have similar diameters. It indicates that the fibril formation may complete within 10 min. Utilizing the crude extract to carry out experiments has a problem. Dissoluted silica remains in the solution, and may initiate the nucleation of the silica deposition process. Therefore, it is not easily to observe the early stages of silica deposition at precise time. At pH 5 and pH 7, silica deposition also generates the similar deposition patterns, fibrils.

Polymerization behavior of silica in aqueous solution has been proposed. In aqueous solution, monosilicic acid condenses to form dimeric, trimeric structures, and then evolve to form particles with size in the nanometer range. When these nuclei form, pH value governs the pattern of further silica deposition. At pH is below 7, particles will aggregate because of weak electrostatic repulsion. Steric and electrostatic effects will force further particle additions taking place at the end of the

elongating chain. And it results a fibril. As fibrils grow, addition can also take place on the side of the chains, and a 3-D network is formed with large water-filled cavities. In contrast, at pH is above 7, electrostatic interaction between charged particles limit the aggregation process. Therefore, particles increase in size and decrease in number.

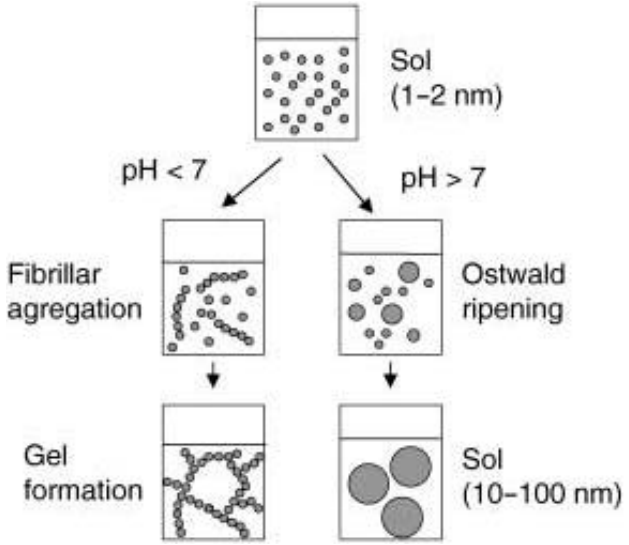

Solid-Gel formation process.

(Adapted form *ChemBioChem* 2003, **4**, 251-259)

Biosilica extract shows a similar but not the same morphology of silica deposition. At pH 3, the morphologies of silica deposition mostly are fibrils and plates. In contrast to the simple aqueous solution, biosilica generates compact fibrils, rather than large water-filled cavities. It indicates that one possible function of these proteins is to overcome the electrostatic or steric effects. It results accelerating fibril aggregation process. Rapid fibrillar aggregation will direct compact fibril rather than a network.

The discontinuous plate may reveal the process of plate formation. Several cross area of the discontinuous plate show a hierarchical organization of the plate

(Figure 13). This plate is made from stacks of thin plates. Each thin plate has the thickness 47.79 nm with the standard deviation 3.07 nm. Moreover, thin plates are composed by one layer of fibril array. These observations indicate that process of plate formation may be hierarchical. One possible process may be: (1) formation of fibrils; (2) aggregating fibrils into one layer array; (3) packing these arrays into stacks.

Special patterns are also observed in our experiments. Figure 14 show objects with bilateral symmetry. The leaf-shaped pattern has a central filament and other fine structures. These leaf-shaped patterns are 2.13 μm in length, and 0.99 μm in width. Also, other pattern with fine structures similar to the leaf-shaped pattern locates together with the leaf-shaped pattern. They are 1.59 μm in length, and 0.34 μm in width. These objects may be the precursor of the leaf-shaped pattern, but the underlying mechanism is unclear.

EDX shows the element compositions of the samples, which deposit silica for 10 min and 20 min. The element compositions are N, C, O, Pt, and Si (with little or none Al signal). These results show that the patterns observed are exact silica deposition.

V. Conclusion

Together with other researches, we may conclude that the organic components in biosilica extract accelerate the silica deposition process, and direct the pattern formations. At pH 3, proteins in biosilica extract may change the microenvironment and initiate silica deposition. Following fibril formation, fibrils form a layer of fibril array and then these arrays aggregate to form stacks. Plates are made from stacks of fibril arrays. Although *in vivo* mechanism is unclear, our results provide a possible way to generate fibril and plate patterns.

We also generate sophisticated leaf-shaped patterns *in vitro*. These results may indicate that self-assembly ability of biosilica extracted proteins will direct pattern formation in vivo. However, the underlying mechanisms are not known.

VI. Figures and Tables

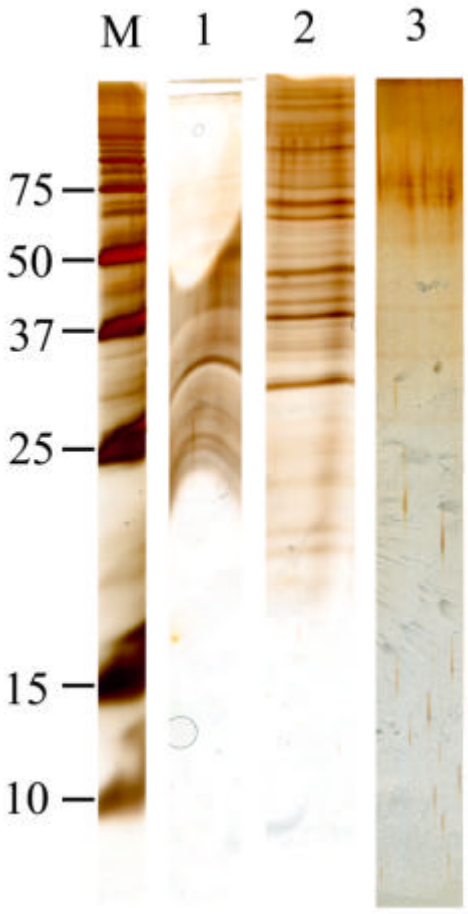

Figure 1. SDS-PAGE. M: markers. 1: Biosilica extracted by 4M HF at 0℃ for 4 hours. 2: Biosilica extrated by 2M HF/ 4M NH_4F at 0℃ for 4 hours. 3: Biosilica extracted as in 2 and then dialyzed against sodium acetate for 24 hours with two exchanges. Dialysis is carried out at 4℃. These components contain proteins, with the molecular weights 70.4, 59.4, 56.8, 46.8, 39.3, 31.2, 27.5, 26.0, 25.0, 22.7, 19.1, 18.0, and 16.1 kDa. Four proteins with dominant quantity are 56.8, 46.8, 39.3, and 31.2 kDa. Small proteins with the molecular weights less than 30 kDa show less quantity.

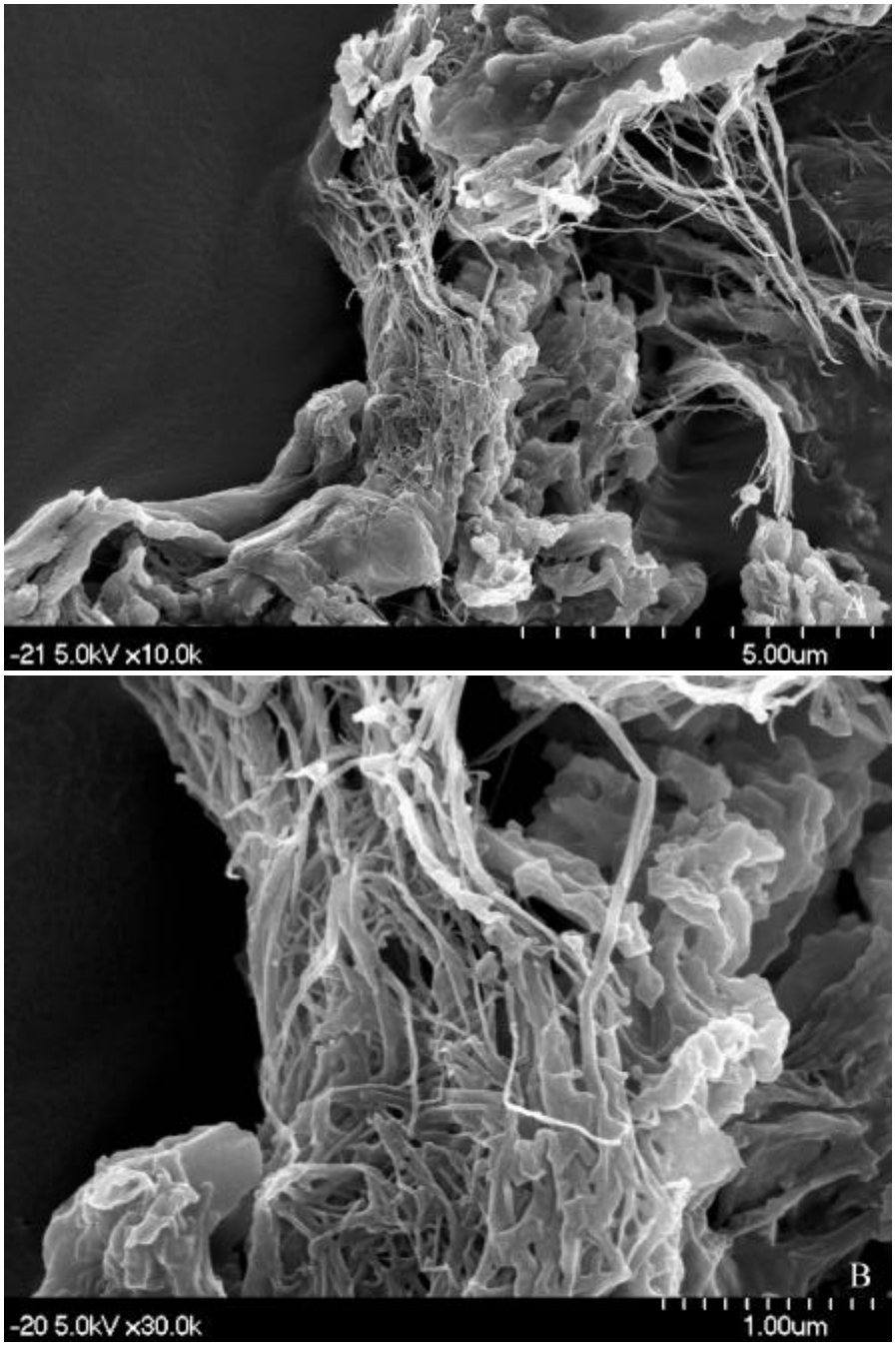

Figure 2. The silica deposition pattern. The extraction is carried out by 2M HF/ 4M NH_4F on ice. The biosilica extract is mixed with 0.01 mM Na_2SiO_3 at pH 3 for 10 min. The dominant pattern is fibrils with 28.67 nm (S.T.D 8.69 nm).

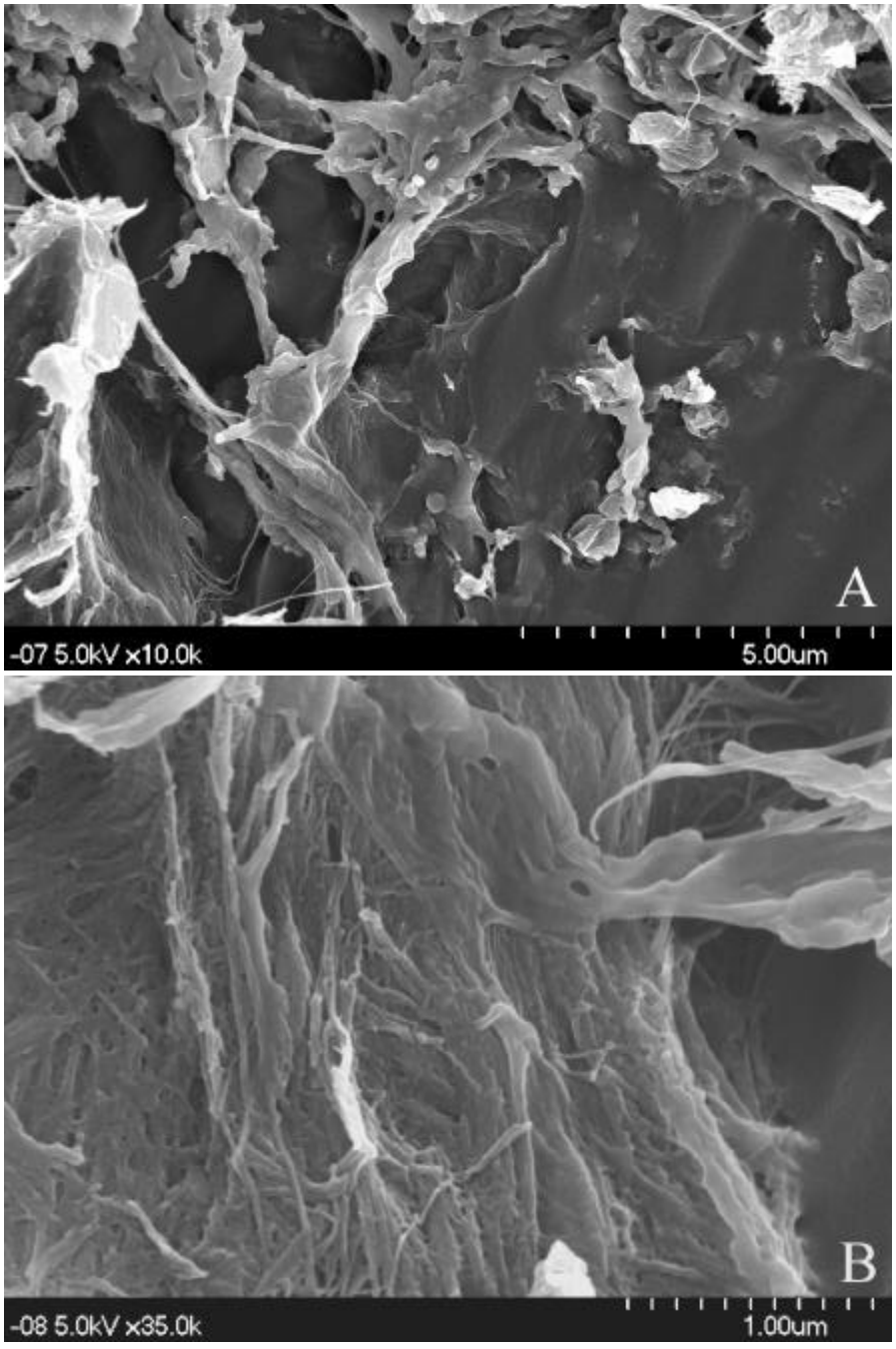
A
-07 5.0kV x10.0k
5.00um
B
-08 5.0kV x35.0k
1.00um

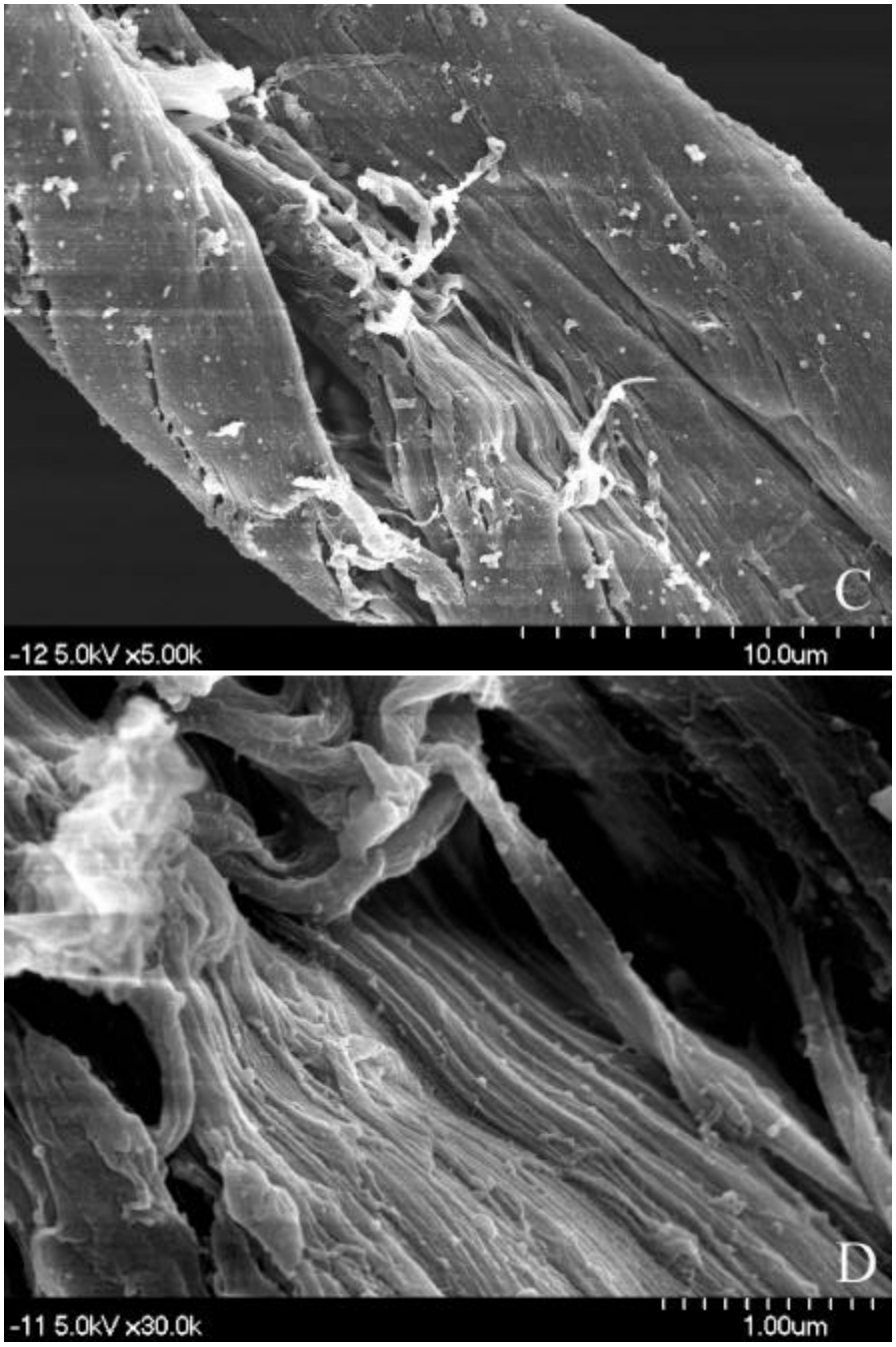

Figure 3. The silica deposition pattern. The extraction is carried out by 2M HF/ 4M NH_4F on ice. The biosilica extract is mixed with 0.01 mM Na_2SiO_3 at pH 3 for 30 min. The dominant pattern is fibrils with 36.00 nm (S.T.D 10.9 nm). Fibrils are aggregated into a larger one (Figure 3C and 3D). The outer surface of the bundle of the fibrils appears a smooth surface.

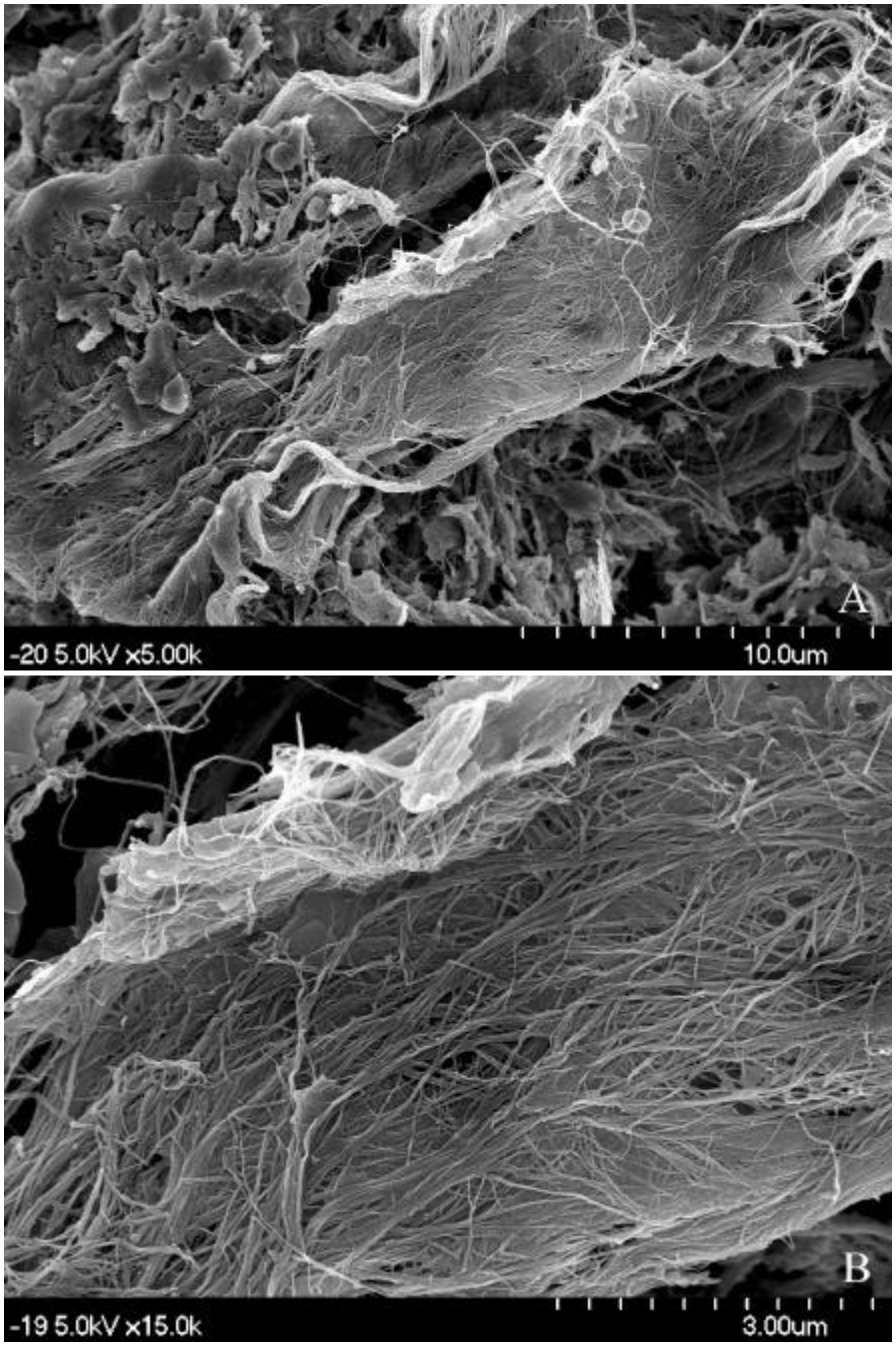
A
-20 5.0kV x5.00k
10.0um
B
-19 5.0kV x15.0k
3.00um

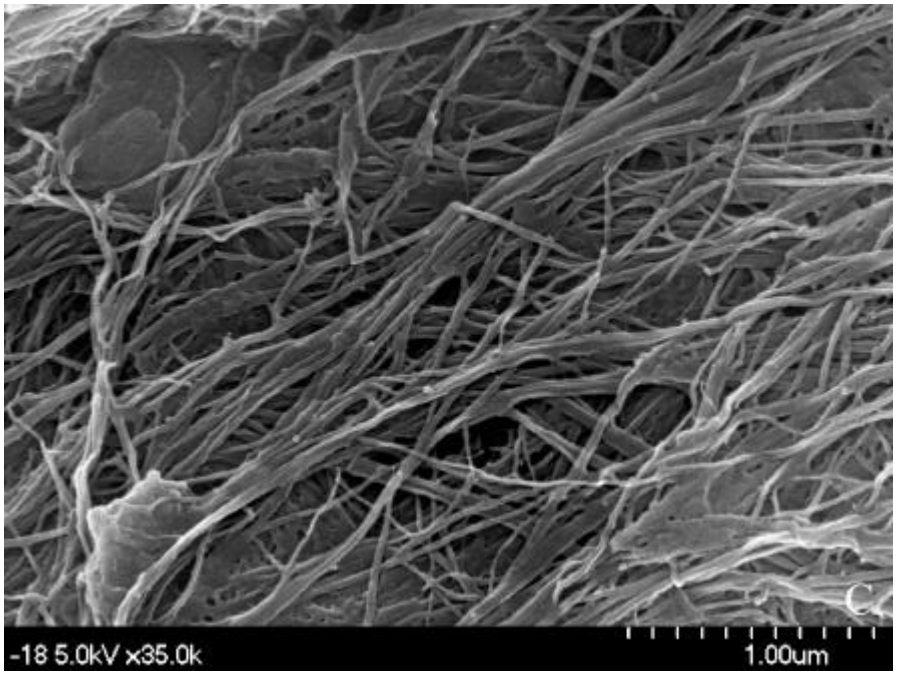

Figure 4. The silica deposition pattern. The extraction is carried out by 2M HF/ 4M NH_4F on ice. The biosilica extract is mixed with 0.01 mM Na_2SiO_3 at pH 3 for 60 min. The dominant pattern is fibrils with 26.20 nm (S.T.D 2.90 nm).

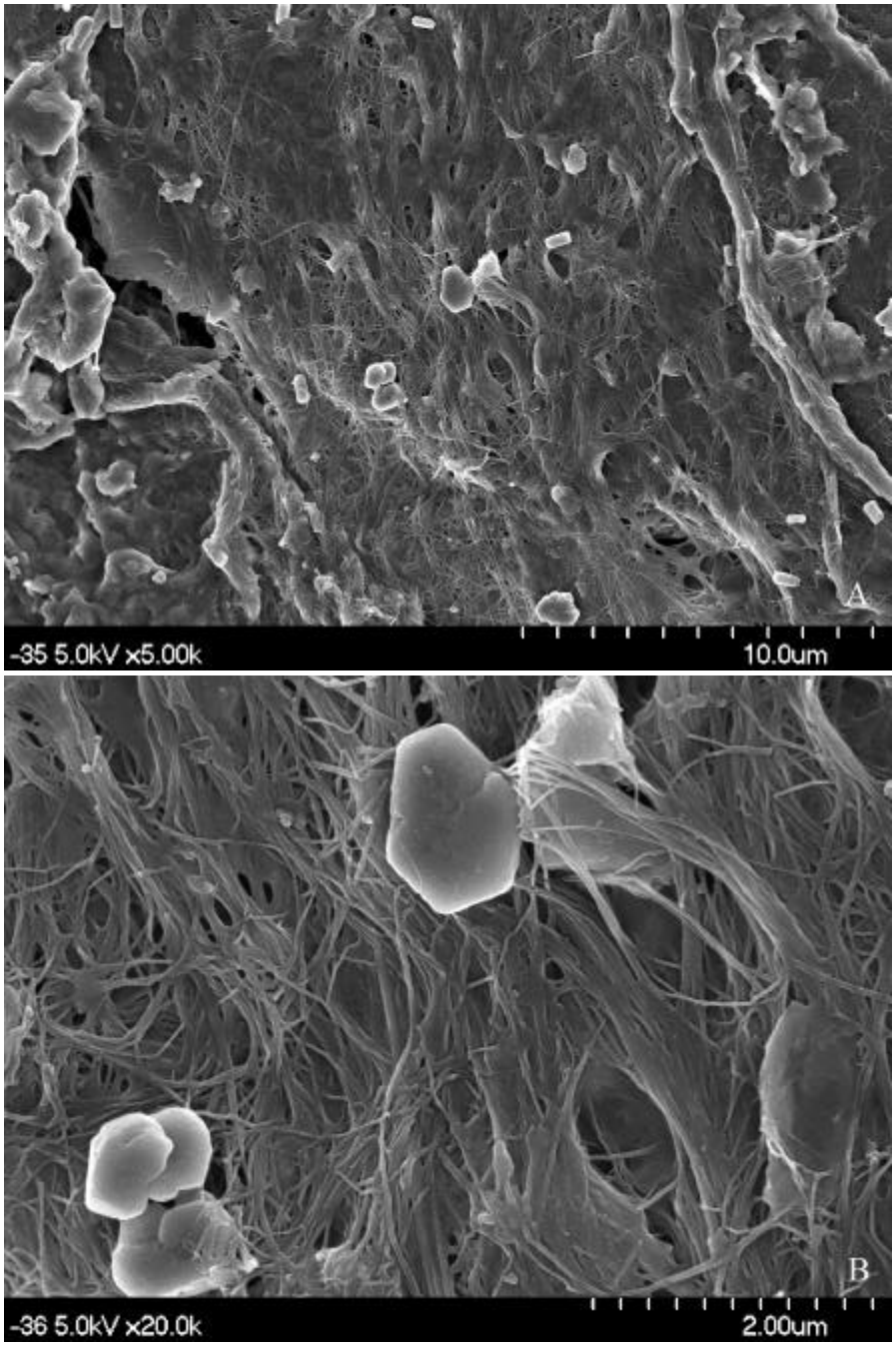
A
-35 5.0kV x5.00k
10.0um
B
-36 5.0kV x20.0k
2.00um

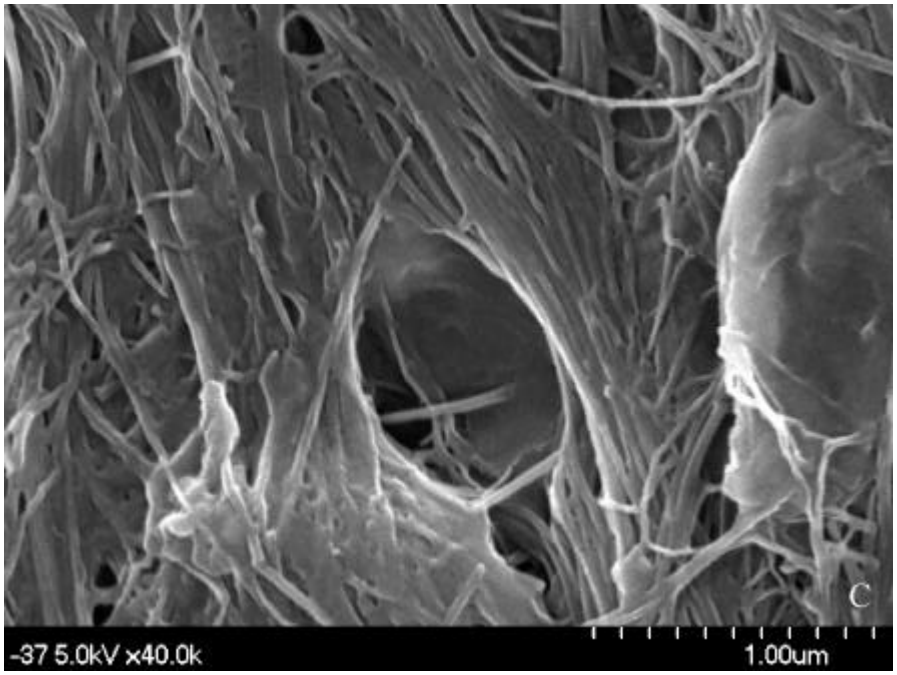

Figure 5. The silica deposition pattern. The extraction is carried out by 2M HF/ 4M NH_4F on ice. The biosilica extract is mixed with 0.01 mM Na_2SiO_3 at pH 3 for 6 hr. The dominant pattern is fibrils with 38.80 nm (S.T.D 10.9 nm). More fibrils are formed along the surface. Irregular particles can be observed (Figure 5A and 5B).

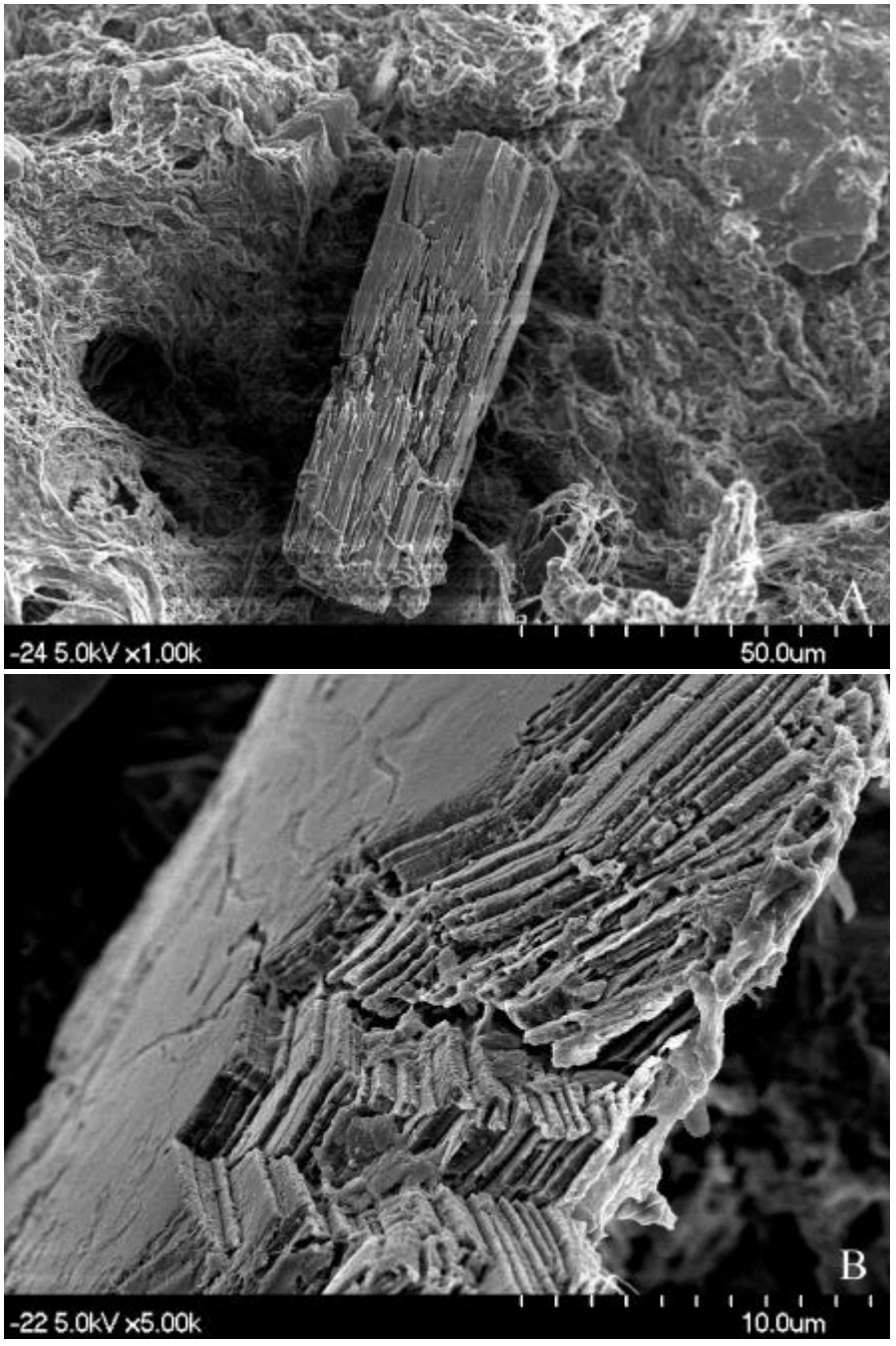
-24 5.0kV x1.00k
50.0um
A
-22 5.0kV x5.00k
10.0um
B

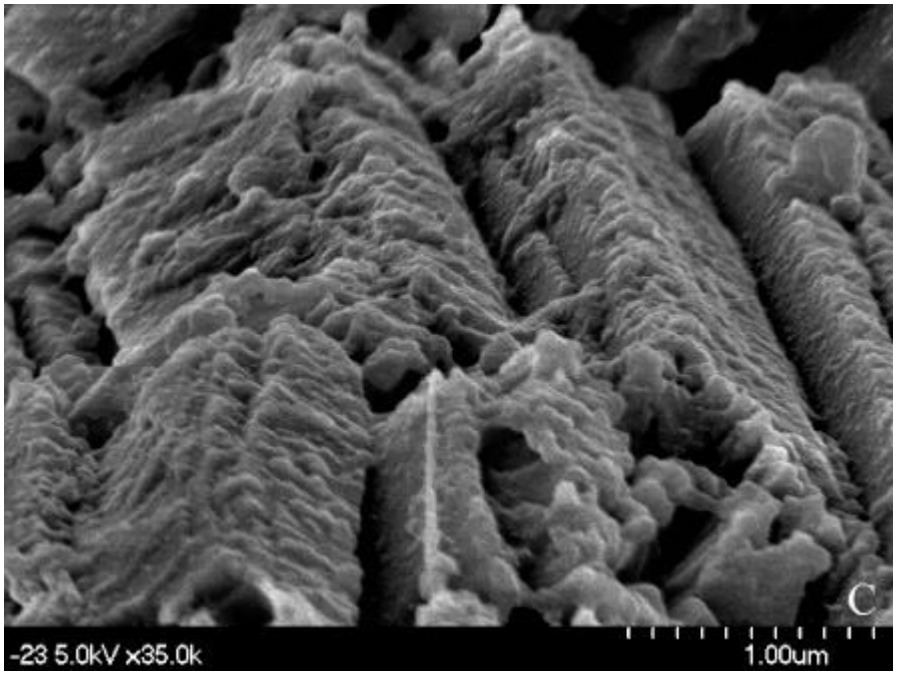

Figure 6. The discontinuous plate. The extraction is carried out by 2M HF/ 4M NH_4F on ice. The biosilica extract is mixed with 0.01 mM Na_2SiO_3 at pH 3 for 24 hr. The discontinuous plate is formed by thin plates, which have the thickness 47.79 nm (STD 3.07 nm) (Figure 6B and 6C). Each plate is composed of fibrils.

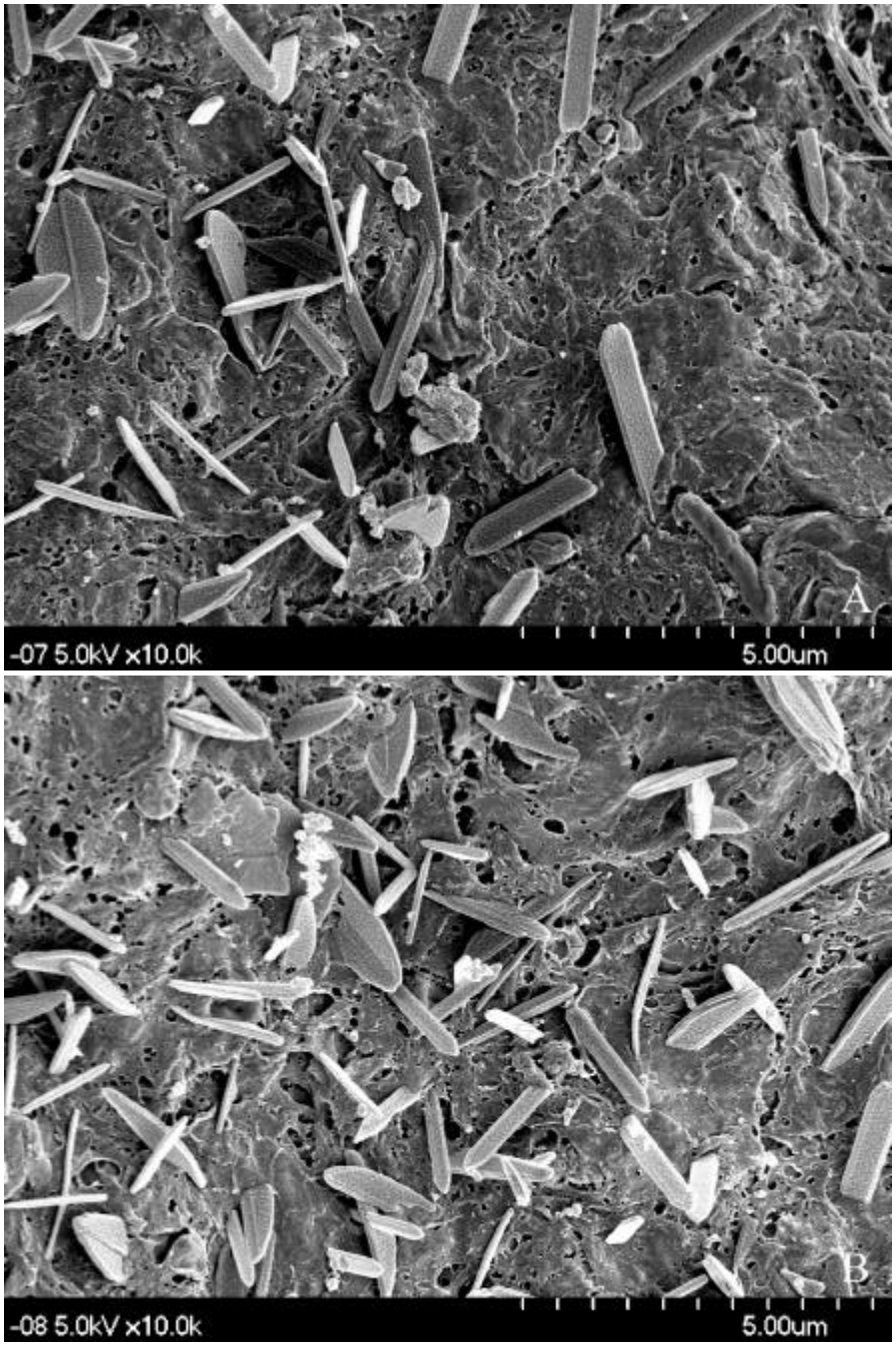

Figure 7. The leaf-shaped pattern. The extraction is carried out by 1M HF/ 2M NH_4F on ice. The biosilica extract is mixed with 0.01 mM Na_2SiO_3 at pH 7. The leaf-shaped pattern has a bilateral symmetry. There are fine structures, such as central vein, on the surface. They are 2.5 μm in length and 0.75 μm in width.

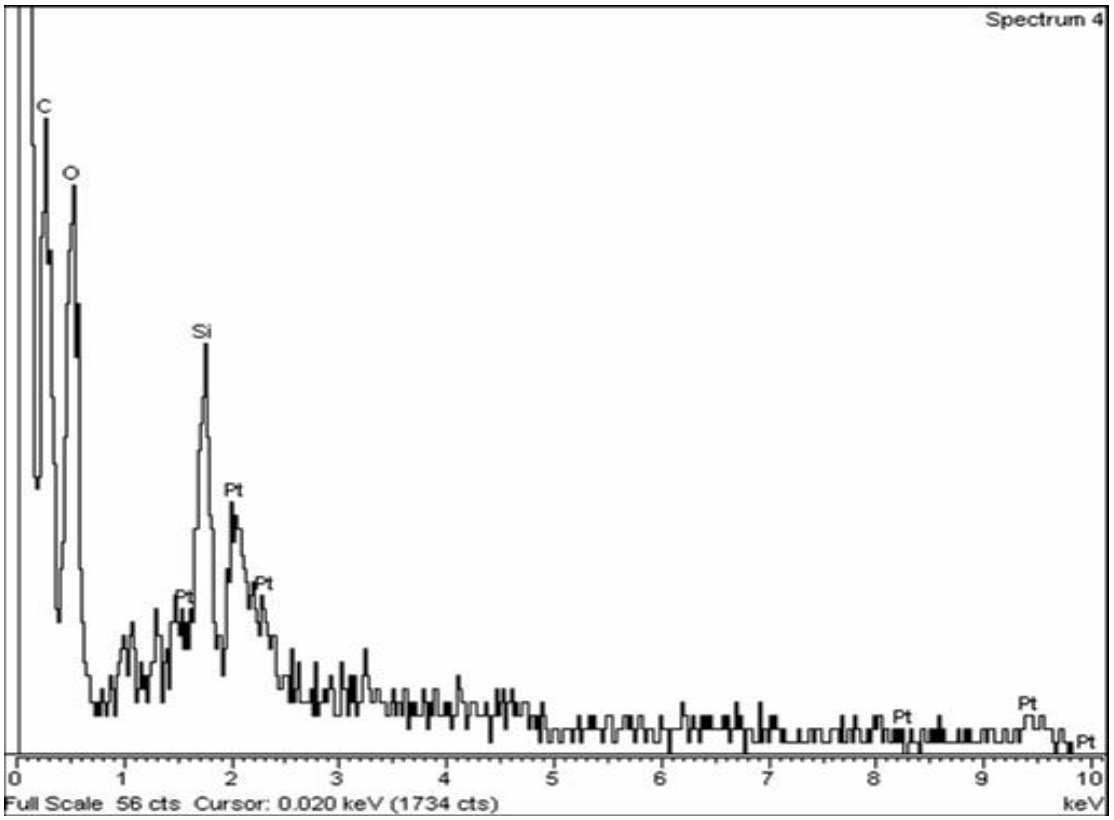

Figure 8. Element composition of the silica deposition determined by EDX. The sample is treated the same condition as Figure 2. There are four dominant signals, C, O, Si, and Pt. No other component signals can be detected. The strong Si signal shows that the sample is the silica deposition.

Table 1. The dry weight of the silica deposition fibrils.

The dry weight of silica deposition has no clear tendency to increase or decrease, since the system error is 0.01133 g. The total amount of silica deposition may be completed within 10 min, and little silica deposition process occurs while deposition time is longer than 10 min.

Time	Dry weight (g)
10 min	0.08323
30 min	0.06387
60 min	0.06007
90 min	0.05835
120 min	0.07753
3 hr	0.05720
6 hr	0.10023

Table 2. The size of the silica deposited fibrils

The samples are prepared with 0.01 mM Na_2SiO_3, pH 3. The diameter of the fibrils does not increase significantly. Since the diameter does not increase significantly, the silica deposited fibrils may be completed with 10 min.

Deposition Time	Diameter (nm)	Standard Deviation
10 min	28.67	8.69
20 min	30.67	2.79
30 min	36.00	10.9
60 min	26.20	2.90
90 min	34.44	7.36
120 min	29.30	3.38
3 hr	25.70	4.81
6 hr	38.80	10.9
9 hr	30.50	8.42
12 hr	28.29	3.92

VII. References

1. Lowenstam H. A. 1981. Minerals formed by organisms. *Science* **211,** 1126-1131.
2. Simpson T. L. and Volcani. B. E. 1981. *Silicon and Siliceous Structures in Biological Systems,* Springer-Verlag
3. Stoermer, E. F., H. S. Pankratz and C.C. Brown. 1965. Fine structure of the diatom *Amphipleura pellucida*. II. Cytoplasmic fine structure and frustule formation. *Amer. J. Bot.* **52,** 1067-1078
4. Reimann, B. E. F., Lewin J. C. and Volcani B. E. 1966. Studies on the biochemistry and fine structure of silica shell formation in diatoms. II. The structure of the cell wall of *Navicula pellculosa* (Brèb) Hilse. *J. Phycol.,* **2,** 74-84
5. Dawson, P. A. 1973. Observations on the structure of some forms of *Gomphonema parvulum* Kütz III. Frustule formation. *J. Phycol.* **9,** 353-365
6. Tippitt, D. H., K. L. McDonald and Pickett-Heaps J. D. 1975. Cell division in the centric diatom *Melosira varians. Cytobiogie,* **12,** 52-76
7. Pickett-Heaps. J. D., K. L. McDonald and Tippit, D.H. 1975. Cell division in the pinnate diatom *Diatoma vulgare*. *Protoplasma,* **86,** 205-242
8. Chiappino, M. L., and Volcani, B. E. 1977. Studies on the biochemistry and fine structure of silica shell formation in diatoms. VII. Sequential cell wall development in the pinnate *Navicula pelliculosa. Protoplasma,* **93,** 205-221
9. Chiara Zurzolo and Chris Bowler. 2001. Exploring Bioinorganic Pattern Formation in Diatoms. A Story of Polarized Trafficking. *Plant Physiol.* **127,** 1339-1345
10. Drum, R. W. 1963. The cytoplasmic fine structure of the diatom, *Nitzschia palea*. *J. Cell Biol.* **18**, 429-440

11. Drum, R. W., Pankratz, H. S. 1964. Post mitotic fine structure of *Gomphonema parvulum*. *J. Ultrastruct. Res*. **10**, 217-223
12. Stoermer, E. F., Pankratz, H. S., Brown, C. C. 1965. Fine structure of the diatom Amphipleura pellucida. II. Cytoplasmic fine structure and frustule formation. *Amer. J. Bot*. **52**, 1067-1078
13. Dawson, P. 1973. Observations on the structure of some forms of *Gomphonema parvulum* Kütz. III. Frustule formation. *J. Phycol*. **9**, 353-365
14. Pickett-Heaps, J. D., Kowalski, S. E. 1981. Value morphogenesis and the microtubule center of the diatom *Hantzschia amphiowys*. Europ. *J. Cell Biol.* **25**, 150-170
15. Borowitzka, M. A., Volcani, B. E. 1978. The polymorphic diatom *Phaeodactylum tricornutum*: Ultrastructure of its morphotypes. *J. Phycol*. **14**, 10-21
16. Schmid, A. M., Schulz, D. 1979. Wall morphogenesis in diatoms: deposition of silica by cytoplasmic vesicles. *Protoplasma* **100**, 267-288
17. Li, C.-W., Volcani B. E. 1985. Studies on the Biochemistry and Fine Structure of Silica Shell Formation in Diatoms VII. Morphogenesis of the Cell Wall in a Centric Diatom, *Ditylum brightwellii*. *Protoplasma* **124**, 10-29
18. Greer, R. G. 1971. The growth of colloidal silica particles. Scanning electron microscopy (part 1). *Proc. 4th Annual Scanning Electron Microscopy Symposium*, pp. 153-160
19. Vocani. B. E. 1981. Cell Wall Formation in Diatoms: Morphogenesis and Biochemistry. In: Simpson T. L. and Volcani. B. E. (ed.). *Silicon and Siliceous Structures in Biological Systems*, Springer-Verlag
20. Schmid, A. M., M. A. Borowitzka and B. E. Volcani. 1981. Morphogenesis and biochemistry of diatom cell walls. In: O. Kiermayer (ed.). *Cytomorphogenesis in Plants*. Springer-Verlan, Vienna.

21. Martin-Jezequel V, Hildebrand M, Brzezinski MA. 2000. Silicon metabolism in diatoms: implications for growth. *J. Phycol.* **36,** 821-840
22. Van Den Hoek C, Mann DG, Johns HM. 1997. *Algae. An Introduction to Phycology*. Cambridge, UK: Cambridge Univ. Press
23. Brzezinski MA, Olson RJ, Chisholm SW. 1990. Silicon availability and cell-cycle progression in marine diatoms. *Mar. Ecol. Prog. Ser.* **67,** 83-96
24. Martin-Jezequel V. Hildebrand M, Brzezinski MA 2000. *J. Phycol.* **36,** 821-840
25. Vaulot D, Olson RJ, Chisholm SW. 1986. Light and dark control of the cell cycle in two phytoplankton species. *Exp. Cell Res.* **167,** 38-52
26. Vaulot D, Olson RJ, Merkel SM, Chisholm SW. 1987. Cell cycle response to nutrient starvation in two marine phytoplankton species. *Mar. Biol.* **95,** 625-630
27. Kröger N, Deutzman R, Sumper M. 1999. Polycationic peptides from diatom biosilica that direct silica nanosphere formation. *Science* **286**, 1129-1132
28. Kröger N, Deutzman R, Bergsdorf C, Sumper M. 2000. Species-specific polyamines from diatoms control silica morphology. *Proc. Natl. Acad. Sci. USA* **97**, 14133-14138
29. Mizutani, T., Nagase, H., Fujiwara, N., Ogoshi, H. 1998 *Bull. Chem. Soc. Jpn*. **71**, 2017-2022
30. Iler, R. K. 1979 *The Chemistry of Silica.* Wiley, New York
31. Gordon, R. and Drum, R. W. 1994. The chemical basis for diatom morphogenesis. *Int. Res. Cytol.* **150,** 243-372
32. Li, C. W., Volcani, B. E. 1984 Aspects of silicification in wall morphogenesis of diatoms. *Philos. Trans. R. Soc. London B* **304**, 519-528
33. Kröger N, Lehmann G, Rachel R, Sumper M. 1997. Characterization of a 200-kDa diatom protein that is specifically associated with a silica-based substructure of the cell wall. *Eur. J. Biochem.* **250,** 99-105

34. Kröger N, Wetherbee R. 2000. Pleuralins are involved in theca differentiation in the diatom *Cylindrotheca fusiformis*. *Protist* **151,** 263-273

35. Kröger N, Bergsdorf C, Sumper M. 1994. A new calcium-binding glycoprotein family constitutes a major diatom cell wall component. *EMBO J.* **13,** 4676-4683

36. Kröger N, Bergsdrof C, Sumper M. 1996. Frustulins: domain conservation in a protein family associated with diatom cell wall. *Eur. J. Biochem.* **239,** 259-264

37. van de Poll WH, Vrieling EG, Gieskes WWC. 1999. Location and expression of frustulins in the pinnate diatoms *Cylindrotheca fusiformis*, *Navicula pelliculosa*, and *Navicula salinarum* (Bacillariophyceae). *J. Phycol.* **35,** 1044-1053

38. Perry CC 1998. In: ed. Interrante LV, Hampden-Smith MJ. *Chemistry of advanced materials: an overview.* Wiley-VCH, New York, 499-562

39. Sumper M. 2002. A Phase Separation Model for the Nanopatterning of Diatom Biosilica. *Science* **295,** 2430-2433.

40. Mann S. 1993. Molecular tectonics in biomineralization and biomimetic materials chemistry. *Nature* **365**, 499-505

41. Oliver, S., Kupermann, A., Coombs, N., Lough, A., and Ozin G. A., 1995. Lamellar Aluminophosphates that Mimic Radiolaria and Diatom Skeletons. *Nature* **378**, 47-50

42. Stöber, W., Fink, A. and Bohn, E. 1968. Controlled growth of monodisperse silica spheres in the micron size range. *J. Colloid Interface Sci.* **26,** 62-69

43. Brinker, C, J. and Scherer, G. W. 1990. *Sol-Gel Science.* Academic, Boston

44. Parkinson, J. and Gordon, R. 1999. Beyond micromachining: the potential of diatoms. *Trends Biotechnol.* **17,** 190-196

45. Mann S, Ozin GA 1996. Synthesis of inorganic materials with complex form. *Nature* **382,** 313-318

46. Morse DE. 1999. Silicon biotechnology: harnessing biological silica production to

construct new materials. *Trends Biotechnol.* **17,** 230-232

47. Parkinson J, Gordon R. 1999. Beyond micromachining: the potential of diatoms. *Trends Biotechnol.* **17,** 190-196
48. Laemmli, U.K. 1970. Cleavage of Structural Proteins during the Assembly of the Head of Bacteriophage T4. *Nature* **227,** 680-685